RESEARCH ARTICLE

Experimental Study of the Combined Effects of Al$_2$O$_3$, CaO and MgO on Gas/Slag/Matte/Spinel Equilibria in the Cu–Fe–O–S–Si–Al–Ca–Mg System at 1473 K (1200°C) and p(SO$_2$) = 0.25 atm

Svetlana Sineva[1] · Denis Shishin[1] · Maksym Shevchenko[1] · Peter C. Hayes[1] · Evgueni Jak[1]

Abstract

The combined effects of Al$_2$O$_3$, CaO and MgO slagging components on phase equilibria and thermodynamics in the basic Cu–Fe–O–S–Si system have been evaluated at 1473 K (1200 °C) and p(SO$_2$) = 0.25 atm for a range of oxygen partial pressures and matte compositions. The experimental technique included high-temperature equilibration of the samples on a spinel substrate under controlled gas atmosphere (CO/CO$_2$/SO$_2$/Ar), followed by rapid quenching and subsequent measurement of the equilibrium phase compositions using Electron Probe X-ray Microanalysis (EPMA). The experimental data have been compared with the results of thermodynamic calculations undertaken using FactSage software and an internal thermodynamic database. Both the experimental results and the calculations results revealed that the presence of Al$_2$O$_3$, CaO and MgO reduced both the sulphur and copper concentrations in the slag phase for a given set of process conditions. The data have been used for further optimisation of the parameters of the thermodynamic database describing multicomponent metallurgical systems. The resulting thermodynamic database is capable of predicting, with high accuracy, the phase equilibria and the distribution of all elements between the phases in the Cu–Fe–O–S–Si–(Al, Ca, Mg) system.

Graphical Abstract
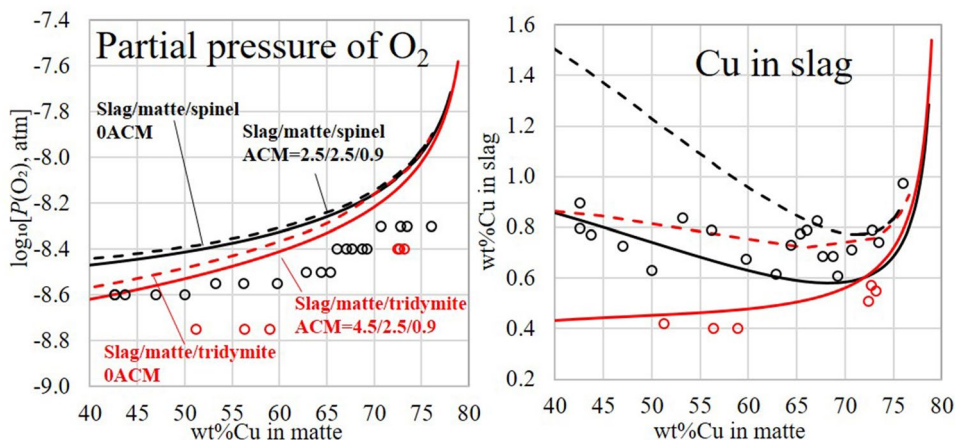
The contributing editor for this article was Markus Reuter.

✉ Svetlana Sineva
  s.sineva@uq.edu.au

Extended author information available on the last page of the article

Introduction

The Cu–Fe–O–S–Si–(Al, Ca, Mg) system describes the principal chemical components present in copper smelting, converting and refining systems. In industrial practice,

fayalite-based copper smelting slags typically contain 2–5 wt% Al_2O_3, 1–4 wt% CaO and 1–2 wt% MgO [1]. These elements are introduced into the processes from concentrates or other feedstocks, fluxing agents and refractory materials, and are distributed between slag, spinel and other solid phases. Accurate quantification of the systems sensitivity to changes in bulk composition and process conditions is highly important for optimization of industrial processes.

The study of the phase equilibria in these complex, high temperature, multi-component, multi-phase systems is a challenging task. The chemical characteristics of slag/matte equilibria and the factors influencing the distribution of major elements between phases have been established in several foundational papers published in the 1950s–70 s of the last century [2–6]. Those studies were focused on the experimental measurement of copper, sulphur, oxygen and minor element distributions between silica-saturated slags and mattes under controlled gas atmospheres. The effects of Al_2O_3 and CaO on the matte/slag phase equilibria were evaluated later [7, 8]. The equilibrium copper and sulphur concentrations in MgO-containing Fe_xO–SiO_2 slags and as well as oxygen concentration in matte at 1300 ºC and $p(SO_2) = 0.1$ atm were measured by Takeda et al. [9, 10]. MgO crucibles were used in both studies but MgO concentration of and Fe/SiO_2 ratio in slags were not fixed at constant values, making it difficult to establish the trends associated solely with MgO concentration.

In all of the above studies, the bulk matte and slag compositions were measured using conventional wet chemical analysis methods, with samples weighing approximately 10 g. Uncertainties associated with this type of technique included potential entrainment of matte in slag phase, difficulties of reaching equilibrium phase compositions in bulk samples within the targeted equilibration time and possible compositional changes during cooling. Using ceramic (i.e. CaO, MgO, Al_2O_3) crucibles resulted in uncontrolled slag composition and inability of a systematical investigation of the fluxing elements effects.

In recent series of studies, an integrated approach combining experimental study and thermodynamic modelling has been implemented to investigate phase equilibria and the distribution of elements in the Cu–Fe–O–S–Si–(Al, Ca, Mg) system [11–18]. The studies of individual and combined effects of Al_2O_3, CaO and MgO on the gas/slag/matte/ tridymite phase equilibria at 1200 and 1300 ºC and $p(SO_2) = 0.25$ atm have been reported by Fallah-Mehrjardi et al. [19] and Sineva et al.[20]. The samples were equilibrated on silica substrates in controlled gas atmospheres at fixed temperatures. The same experimental technique with spinel substrates has been used to measure the individual effects of Al_2O_3, CaO and MgO for gas/slag/matte/spinel phase equilibria at 1200 ºC and $p(SO_2) = 0.25$ atm [21]. Similar research focused on study of MgO and CaO effect on

gas/slag/matte/spinel at slightly different $p(SO_2) = 0.3$ atm with experimental technique adopted from [15] has been published in papers [22–24].The latest research of individual effects of Al_2O_3 and CaO on distribution of major elements between slag and matte phases in equilibrium with spinel at $p(SO_2) = 0.25$ atm and 1250 ºC have been reported in doctoral thesis of Min Chen [25]. Thermodynamic modelling of the effects of Al_2O_3, CaO and MgO on slag/matte equilibria in the Cu–Fe–O–S–Si–(Al, Ca, Mg) system was carried out by Shishin et al. [26]. The model reproduced individual effects of Al_2O_3, CaO and MgO on slag/matte phase equilibria on spinel and tridymite substrates. The combined effects of $Al_2O_3 + CaO + MgO$ on slag/matte/spinel equilibria for high Fe/SiO_2 have not been accurately measured to date. The aim of the present paper is to fill that gap, producing accurate experimental measurements of combined Al_2O_3, CaO and MgO effects on the gas/slag/matte/spinel phase equilibria at 1200 ºC and $p(SO_2) = 0.25$ atm for a range of oxygen partial pressures and matte compositions.

Experimental Study

Overall Description of the Experimental Technique

The experimental technique used in the present study involved high-temperature equilibration of slag and matte phases using spinel substrates in controlled gas atmospheres (CO/CO$_2$/SO$_2$/Ar), quenching of the equilibrated sample and accurate measurement of the compositions of coexisting phases using Electron Probe X-ray Microanalysis (EPMA). The technique has been developed for accurate measurement of the phase equilibria in the multicomponent systems at high temperatures. Application of EPMA for determination of the compositions of phases presented in equilibrated slag/matte samples eliminated the possibility of measuring entrained droplets or solids since the phases were readily distinguished. Combining EPMA with SEM enabled the selection of areas in which all equilibrium phases were in close association and accurate measurement of the compositions of coexisting phases. Low weight of the samples, 0.3–0.5 g, ensured the achievement of equilibrium within a reasonable experimental time and enabled rapid quenching after equilibration process. Applying the primary phase as a substrate for matte/slag/gas equilibria prevented contamination of the sample by side elements that could be associated with crucible materials. The sample mixture compositions and process conditions used in each experiment were calculated using the thermodynamic database, thus decreasing the overall number of experiments required to accurately characterise the system and to determine the optimum values of the database model parameters.

Possible uncertainties arising from the technique used could be related to experimental errors, arisen from the equilibration experiments fulfillment and uncertainties of EPMA measurements. The possible uncertainties as well as potential ways of overcoming them at applying the discussed technique are listed below.

Experimental Uncertainties

- The presence of impurities in the initial reagents and possible contamination during mixture and sample preparation. Potential side impurities were detected and controlled by measuring EDS (energy dispersion spectra) of samples following equilibration.
- Uncertainties of high-temperature equilibration:
- Temperature uncertainties (location of the sample relative to hot zone, thermocouple errors, gradual contamination and disintegration of thermocouples during their use) were minimised by thermocouple calibration against standard thermocouple supplied by Australian Standards Laboratory and periodic measurements of the temperature profile of the furnace.
- Gas composition uncertainties include initial gas purity, mixing ratio of gases, possible minor cracks and leakages in the connections, blockage of furnace with sulphur precipitates. The flowrates of high purity gases were controlled by calibration of the flowmeters. Generated oxygen partial pressures were cross-checked using an oxygen probe. Several experiments were repeated to ensure reproducibility of $p(O_2)$ vs matte grade curve.

To ensure complete achievement of equilibrium a "4-point test" approach was applied involving examination of the effects of the equilibration time, homogeneity within the individual phases, approach to equilibrium from different starting conditions and analysis of the reaction sequence taking place during equilibration. Details of the "4-point test" approach can be found in [18].

- Compositional changes in the phases during quenching were minimised by selection of well-quenched areas and appropriate probe diameter for measurement.

Uncertainties of EPMA Measurement

- Thickness and uniformity of carbon coating of the samples and standards were controlled by introducing standard carbon coating parameters.
- Surface condition (smoothness, pores/cracks, oxidation/hydration) of the samples was controlled by maintaining clean work environment and special conditions of the samples storage and reporting totals before normalisation.

- Uncertainties in EPMA standards for given measurement session were avoided by repeated measurement of standards as unknowns during the session, using the pure components or stoichiometric phases observed in samples to recheck the standards, and, where possible, by mounting small standard particles in the sample block.
- Selection of the appropriate measurement location and number of measured points was carried out by examination of different areas of the sample by SEM.
- Uncertainties in ZAF correction were controlled by selecting standards close to compositions of the samples and using secondary stoichiometric standards for testing.
- Effect of secondary fluorescence (manifested as apparent solubility of certain elements in a particle that has no or lower real solubility of that element, but is surrounding by a matrix containing that element) was corrected by a blank unreacted couple test, and where appropriate by changing other energy of measured characteristic line for the same element (for instance, changing from K to L characteristic line for some elements) [27, 28].

Experimental Technique

The first step of experiments preparation was aimed to prediction the appropriate initial mixture compositions at fixed conditions using FactSage software [29] and the current version of the confidential thermodynamic database for FactSage developed by Pyrosearch innovation centre (The University of Queensland) [12, 30]. The principal objectives of the calculations were to estimate the phase ratios at selected $p(SO_2)$, $p(O_2)$, temperature and matte grade. The slag/matte/spinel mass ratios used in the experiments were approximately 0.6/0.3/0.1, respectively. The initial mixtures were prepared from metal, sulphide and oxide powders: precalcined SiO_2 (99.9 wt% purity), Cu_2S (99.5 wt% purity), FeS (99.9 wt% purity), $FeO_{1.05}$ (99.9 wt% purity), Fe (99.9 wt% purity), Cu (99.9 wt% purity), MgO (99.99 wt% purity), Al_2O_3 (99.99 wt% purity) supplied by Alfa Aesar (MO, USA). The CaO was added to the system in the form of preliminary synthesised "master slag" with composition of 60 mol.% SiO_2–40 mol.% CaO. The master slag was prepared from calcined SiO_2 and $CaCO_3$ at required weight ratio in an open silica ampoule at 1400 °C in a muffle furnace overnight, cooled slowly, and contained a mixture of wollastonite $CaSiO_3$ and quartz or tridymite SiO_2 as confirmed by SEM. The typical examples of the initial mixtures with different ratio of initial reagents targeted for fixed oxygen partial pressure are given in Table 1.

The oxide, sulphide and metal powders in preset ratios were thoroughly mixed, pelletised and placed on a spinel (magnetite) substrate. The average weight of the samples was approximately 0.3–0.5 g. The spinel (Fe_3O_4) substrate was prepared through oxidation of pure iron foil (99.99 wt%

Table 1 Initial mixtures and conditions of equilibration experiments

# Mixture	Weight of initial components (g)							log P(O_2), atm	Gas flow ratio (ml/min)			Slag/matte/spinel ratio
	Cu_2S	FeS	SiO_2	Fe_2O_3	CaSiO3	MgO	Al_2O_3		SO_2	80Ar/20CO	CO_2	
1	0.28	0.00	0.17	0.47	0.03	0.01	0.03	− 8.3	127.7	92.4	279.8	0.55/0.32/0.12
2	0.24	0.05	0.15	0.49	0.03	0.01	0.03	− 8.4	129.1	111.0	260.0	0.56/0.35/0.09
3	0.21	0.05	0.15	0.51	0.03	0.01	0.03	− 8.5	136	131.1	232.9	0.51/0.46/0.03
4	0.16	0.02	0.14	0.58	0.03	0.01	0.03	− 8.55	135.2	150.4	215.0	0.52/0.43/0.05
5	0.13	0.00	0.13	0.66	0.04	0.01	0.04	− 8.6	134.4	170.9	194.7	0.53/0.40/0.07

purity) at 1200 ℃ in CO_2 atmosphere for 2 h. Various shapes of spinel substrates were tested by Hidayat et al. [15]. The final type of substrate was adopted in the form of rectangular basket with an open bottom. The schematic illustration of spinel basket, photo of oxidised spinel with size dimensions as well as photo of mounted spinel with sample inside are shown in Fig. 1.

The spinel substrate containing the experimental sample was suspended in a 32 mm ID recrystallised alumina reaction tube and positioned in the calibrated, uniform hot zone of a vertical, electrically heated furnace at a given temperature, 1200 ℃. The sample temperature was measured by an alumina-shielded and calibrated Pt/Pt-13 wt% Rh thermocouple placed immediately adjacent to the sample. Digital 4-channel multimeter TM-947SD manufactured by Lutron electronic (Taiwan) with data logger from SD card was connected to thermocouple for temperature measurement. The sample temperature was estimated to be within ± 5 ℃ of the target value.

The constant p(SO_2) = 0.25 atm and oxygen partial pressures, p(O_2) in the range of $10^{-8.3}$–$10^{-8.6}$ atm were maintained by an accurate control of the CO, CO_2, SO_2, and Ar ratios in the gas phase using a system of calibrated U-tube capillary flow-meters. Totally 5 different oxygen partial pressures for experimental mixtures were targeted: $10^{-8.3}$, $10^{-8.4}$, $10^{-8.5}$, $10^{-8.55}$, $10^{-8.6}$ atm (see details in Table 1). The aim of the proposed experimental plan was to reach the equilibrium state from different directions (from higher or lower copper concentration in matte phase). It was assumed that for the same mixture directions of the main reactions can be shifted depending on oxidation potential in the gas phase. Detailed analysis of the potential reactions during the gas/slag/matte/spinel equilibration process was published by Hidayat et al. [15]. The desired flowrates of gases to achieve the selected conditions were calculated using FactSage FactPC database for the ideal gas phase [29]. The accuracies of the oxygen potentials produced by the sulphur-free gas mixtures were confirmed by flowing the mixtures through a separate vertical tube furnace equipped with a DS-type oxygen probe (supplied and calibrated by Australian Oxygen Fabricators, AOF, Melbourne, Australia) operated at the same temperature as used in the experiments.

Several preliminary tests were carried out for 0.5, 1, 6, 18, 24, and 48 h to determine the required experiments duration. Detailed explanation of the technique for determination of the proper equilibration time for experiments in equilibrium with gas phase was published earlier [15]. Based on that technique and analysis of the results obtained the final experimental time was selected to be between 20 and 24 h, which allows the phases of the system to reach thermodynamic equilibrium. All samples were then directly quenched
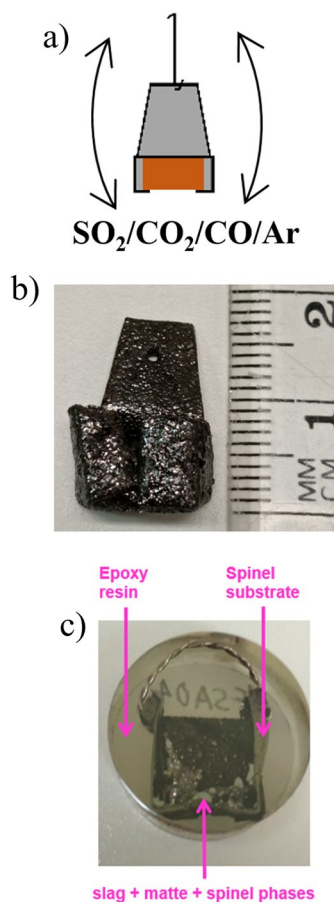

Fig. 1 Schematic illustration (**a**), photo of the spinel substrate (**b**), and photo of mounted spinel with sample inside (**c**)

in brine solution (20 wt% of $CaCl_2$ in water kept at -20 ℃) to capture the equilibrium phase compositions at 1200 ℃.

The quenched samples were washed, dried, mounted in the epoxy resin and polished using Tegramin polishing machine, manufactured by Struers (Denmark) for further examination.

Direct measurement of the equilibrium phase compositions was undertaken by electron probe X-ray microanalysis (EPMA) using the JEOL JXA 8200L probe (trademark of Japan Electron Optics Ltd., Tokyo) at an acceleration voltage of 15 kV and a probe current of 20 nA. $K\alpha_1$ characteristic lines were selected for Cu (LIF crystal[1]), Fe (LIF crystal), S (PET crystal1), Si (TAP crystal11), Ca (PET crystal), Mg (TAP crystal) and Al (TAP crystal) concentrations measurements. Appropriate reference materials from Charles M. Taylor, Stanford, CA were used as standards. Cu and Fe in matte phase were calibrated against pure Cu and Fe metals, S was calibrated against chalcopyrite standard ($CuFeS_2$). For slag and spinel phases, standard materials Cu metal, Fe_2O_3, SiO_2, $CaSiO_3$, MgO and Al_2O_3 were used to calibrate Cu, Fe, Si, Ca, Mg, and Al, respectively. Fe_2O_3 was used as the oxygen standard for direct measurements of oxygen in the matte phase. The detailed technique of oxygen measurement in matte phase was described in [25]. Briefly, oxygen concentration in matte was measured using the $K\alpha$ line by an LDE1 spectrometer crystal1, specially designed for measuring of light elements. The signal collection times for peak and background were 40–50 s. and 6–8 s, respectively, depending on the estimated oxygen concentration in the phase. The Duncumb–Philibert ZAF correction procedure[2] supplied with the JEOL JXA 8200L probe software was applied to the data obtained. The standard ZAF correction was further improved for the fayalite slag compositions, following an approach described in [28, 31].

For slag and spinel phases, measured metal cations were recalculated to selected oxidation states (Cu_2O, FeO, SiO_2, Al_2O_3, CaO and MgO) for presentation purposes. The

Fig. 2 Back-scattered electron micrographs of Cu–Fe–O–S–Si–Al–Ca–Mg system illustrating the typical sample microstructures of gas/slag/matte/spinel equilibria **a** Sample # 5 from Table 2; **b** Sample # 14 from Table 2

obtained results were listed in a tabular form with indicated initial sum of elements before normalisation.

Results

Figure 2 illustrates the typical sample microstructures, containing matte, slag and spinel phases adjacent to and in equilibrium with the gas phase. It can be seen that all phases are homogeneous and well quenched. The cross-sections of the matte phase are typically in the range of 10–300 μm diameter, and compositions of the matte droplets larger than 50 μm were measured. The slag phase compositions were measured in close proximity to matte and spinel phases, but not closer than 20 μm from phase boundaries so as to avoid any effect of secondary fluorescence. Spinel grains, typically 10–50 μm diameter, were randomly distributed in the slag phase.

The EPMA measured compositions of the phase present in the equilibrated samples are listed in Table 2. The concentrations of Al_2O_3, MgO and CaO in the matte phase are below detection limits and therefore are not reported. The concentrations of Cu and S dissolved in spinel phase are close to the EPMA detection limit and do not exceed 0.1 wt. % for the majority of the samples. The concentrations

---

[1] LDE1, TAP, PET, and LIF are all different types of crystals that are used to cover the entire X-ray spectrum in EPMA. Lithium fluoride (LIF), pentaerythritol (PET), thallium acid pthalate (TAP), and artificial layered dispersive element (LDE) crystals are the most commonly used. LDE1 and TAP crystals are used for light-elements (low-energy) analysis, while PET and LIF crystals, in conjunction with the TAP crystals, cover the heavier elements.

[2] ZAF correction means a mathematical correction of raw X-ray data that takes into account the following three effects on the characteristic X-ray intensity when performing quantitative analysis: 1) atomic number (Z) effect, 2) absorption (A) effect, and 3) fluorescence excitation (F) effect. ZAF is the abbreviation of the effects. The ZAF correction procedure is an important step in quantitative X-ray microanalysis, which is used to determine the elemental composition of samples at high spatial resolutions. The procedure allows for accurate quantification of X-ray spectra, enabling researchers to obtain reliable elemental concentrations from samples.
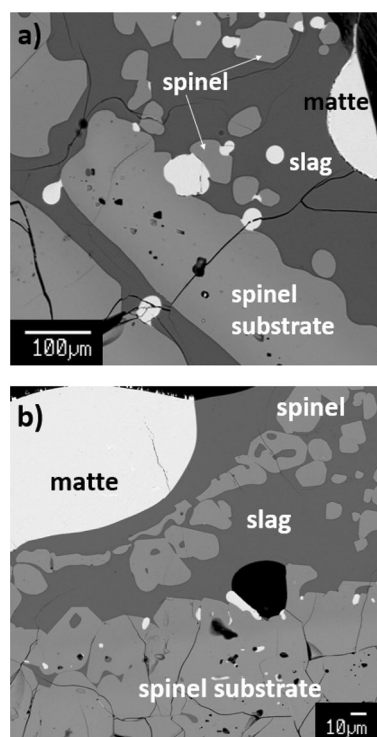
Table 2 EPMA measured compositions of the phases at the slag/matte/metal/spinel equilibria in the Cu–Fe–O–S–Si–Al–Ca–Mg system at 1473 K (1200 °C) and p(SO₂)=0.25 atm (24 h equilibration time)

No	Log₁₀ [p(O₂), atm]	Normalized Matte Composition (wt%)				Total	Phase	Normalized oxide composition (wt%)							Total	Cu in slag (wt%)	Fe/SiO₂ in slag
		Cu	Fe	S	O			Cu₂O	FeO/Fe₃O₄	SiO₂	S	Al₂O₃	CaO	MgO			
1	−8.6	42.6±1.3	28.4±1.0	26.1±0.5	2.8±0.2	98.5	Slag	1.0±0.1	67.4±0.5	24.5±0.8	3.0±0.2	1.6±0.1	1.8±0.07	0.7±0.05	98.8	0.89	2.1
							Spinel	0.02±0.01	95.5±0.2	0.6±0.06	0.0	3.6±0.2	0.0	0.3±0.04	98.3		
2	−8.6	40.9±1.4	29.6±0.9	25.6±0.6	3.9±0.5	98.3	Slag	0.96±0.08	66.2±0.2	24.6±0.2	2.7±0.1	2.3±0.1	2.6±0.03	0.7±0.03	99.1	0.8	2.1
							Spinel	0.01±0.01	95.6±0.2	0.6±0.1	0.0	3.2±0.1	0.0	0.3±0.09	98.7		
3	−8.6	43.7±1.7	27.3±1.5	26.5±0.5	2.4±0.3	97.7	Slag	0.87±0.2	65.9±0.9	26.2±0.9	2.3±0.2	1.7±0.3	2.4±0.1	0.7±0.05	98.7	0.77	2.0
							Spinel	0.06±0.04	97.1±0.5	0.6±0.04	0.0	2.0±0.4	0.0	0.3±0.04	98.0		
4	−8.6	45.7±1.1	25.8±0.9	25.8±0.3	2.7±0.2	98.5	Slag	0.82±0.1	65.7±0.4	25.0±0.5	2.6±0.2	2.6±0.2	2.6±0.1	0.7±0.05	100.1	0.73	2.0
							Spinel	0.07±0.03	97.2±0.6	0.2±0.05	0.0	2.2±0.3	0.0	0.3±0.04	99.8		
5	−8.6	49.2±0.7	23.4±0.7	25.7±0.1	1.8±0.1	98.2	Slag	0.71±0.05	65.1±0.9	25.9±0.9	2.2±0.3	2.1±0.3	3.1±0.2	0.8±0.05	99.6	0.63	2.0
							Spinel	0.05±0.03	97.9±0.8	0.4±0.1	0.0	1.4±0.2	0.0	0.3±0.05	100.8		
6	−8.55	53.2±0.7	19.3±0.6	25.8±0.4	1.7±0.2	98.8	Slag	0.91±0.06	66.3±0.2	26.8±0.3	2.2±0.1	1.1±0.05	2.3±0.03	0.3±0.04	98.9	0.84	1.9
							Spinel	0.01±0.01	97.0±0.4	0.7±0.1	0.0	2.1±0.5	0.0	0.1±0.05	97.9		
7	−8.55	56.3±1.8	18.9±1.1	24.9±0.7	1.2±0.1	99.6	Slag	0.89±0.1	64.0±0.3	27.6±0.2	1.5±0.09	3.1±0.1	2.0±0.02	0.8±0.04	98.9	0.79	1.8
							Spinel	0.04±0.03	98.7±0.3	0.6±0.1	0.0	0.6±0.2	0.0	0.1±0.04	98.8		
8	−8.55	59.8±1.2	15.8±0.8	24.5±0.5	n/a	99.9	Slag	0.77±0.06	63.4±0.4	28.7±0.3	1.3±0.06	2.8±0.4	2.0±0.03	1.0±0.07	99.9	0.67	1.7
							Spinel	n/a	n/a	n/a	n/a	n/a	n/a	n/a	n/a		
9	−8.5	62.9±0.6	11.9±0.4	24.3±0.3	0.9±0.1	98.9	Slag	0.69±0.03	60.8±0.2	31.3±0.2	1.0±0.03	2.9±0.1	2.3±0.05	1.0±0.1	98.4	0.62	1.5
							Spinel	0.1±0.01	94.6±0.7	0.6±0.04	0.0	4.2±0.7	0.0	0.3±0.04	98.7		
10	−8.5	64.4±0.9	11.9±0.7	23.7±0.4	0.1	99.9	Slag	0.83±0.06	60.1±1.5	31.7±0.6	1.0±0.1	2.9±0.4	2.5±0.1	1.1±0.1	98.6	0.73	1.5
							Spinel	0.1±0.05	91.9±1.0	0.6±0.06	0.0	6.7±0.9	0.0	0.5±0.1	99.6		
11	−8.5	64.9±0.9	11.6±1.2	22.7±0.9	0.8±0.1	99.2	Slag	0.88±0.09	60.2±0.2	31.3±0.3	1.0±0.06	3.1±0.1	2.3±0.05	1.1±0.02	100.4	0.77	1.5
							Spinel	0.03±0.02	97.7±0.9	0.4±0.2	0.0	2.3±0.7	0.0	0.2±0.1	98.3		
12	−8.4	66.1±0.6	10.9±0.9	23.0±0.7	n/a	100.2	Slag	0.89±0.07	62.2±0.4	30.0±0.4	1.2±0.05	2.4±0.1	2.7±0.05	0.5±0.02	100.2	0.79	1.6
							Spinel	n/a	n/a	n/a	n/a	n/a	n/a	n/a	n/a		
13	−8.4	67.1±0.4	9.8±0.6	23.1±0.5	n/a	99.8	Slag	0.93±0.07	62.4±0.3	30.4±0.3	0.9±0.04	2.2±0.05	2.2±0.05	0.9±0.03	100	0.83	1.6
							Spinel	n/a	n/a	n/a	n/a	n/a	n/a	n/a	n/a		
14	−8.4	67.0±0.3	9.6±0.4	22.4±0.2	1.0±0.1	99.8	Slag	0.77±0.08	64.1±0.2	30.6±0.2	0.8±0.03	2.4±0.1	2.2±0.03	0.8±0.04	100.6	0.68	1.6
							Spinel	0.03±0.02	93.9±0.4	0.6±0.2	0.0	5.1±0.4	0.0	0.3±0.03	100.7		
15	−8.4	68.8±0.3	7.4±0.2	23.2±0.2	0.6±0.1	99.3	Slag	0.77±0.09	63.2±0.4	31.4±0.4	0.8±0.05	1.6±0.1	1.9±0.07	0.4±0.04	98.1	0.68	1.6
							Spinel	0.05±0.04	96.7±0.1	0.7±0.05	0.0	2.3±0.1	0.0	0.1±0.02	99.5		
16	−8.4	69.2±0.5	7.6±0.5	22.5±0.3	0.7±0.1	99.1	Slag	0.69±0.07	57.3±0.5	34.1±0.6	0.5±0.04	3.9±0.2	2.5±0.1	1.2±0.05	99.2	0.61	1.3
							Spinel	0.10±0.05	94.3±0.5	0.6±0.01	0.0	4.6±0.5	0.0	0.3±0.04	99.5		
17	−8.3	70.7±0.2	7.3±0.1	22.0±0.2	0.3±0.1	99.8	Slag	0.8±0.09	58.4±0.6	33.5±0.3	0.5±0.02	3.2±0.2	2.5±0.2	0.9±0.08	100.4	0.71	1.4
							Spinel	0.07±0.06	96.5±0.4	0.6±0.04	0.0	2.7±0.3	0.0	0.1±0.06	n/a		

Table 2 (continued)

No	$\log_{10}$ [p(O_2), atm]	Normalized Matte Composition (wt%)				Total	Phase	Normalized oxide composition (wt%)							Total	Cu in slag (wt%)	Fe/SiO_2 in slag
		Cu	Fe	S	O			Cu_2O	FeO/Fe_3O_4	SiO_2	S	Al_2O_3	CaO	MgO			
18	−8.3	72.8±0.2	5.6±0.1	21.6±0.2	0.4±0.1	99.2	Slag	0.89±0.09	57.0±0.5	33.7±0.3	0.3±0.02	4.4±0.2	2.6±0.05	1.1±0.06	98.3	0.79	1.3
							Spinel	0.12±0.06	97.8±0.7	0.7±0.1	0.0	4.2±0.3	0.0	0.3±0.05	99.6		
19	−8.3	73.5±0.2	4.9±0.1	21.6±0.1	0.4±0.04	97.8	Slag	0.83±0.04	55.8±0.4	34.7±0.2	0.3±0.02	4.4±0.2	2.7±0.05	1.1±0.09	98.4	0.74	1.3
							Spinel	0.02±0.01	97.9±0.4	0.7±0.1	0.0	3.3±0.3	0.0	0.2±0.06	100.6		
20	−8.3	76.1±0.8	1.9±0.2	21.8±0.6	0.2±0.09	97.9	Slag	1.1±0.1	58.3±0.9	35.4±0.6	0.2±0.03	2.2±0.3	2.3±0.07	0.5±0.06	98.8	0.97	1.3
							Spinel	0.07±0.07	97.1±0.3	0.6±0.06	0.0	2.1±0.2	0.0	0.1±0.03	98.3		

of chemically dissolved copper and Fe/SiO_2 ratios in slag are also given in Table 2. The column "EPMA Total" refers to unnormalised sum of elemental concentrations measured by EPMA.

The experimental data were plotted on a set of graphs with copper concentration in matte phase (wt% Cu) on the X-axis. The graphs presenting p(O_2), p(S_2), p(SO_2); S and O concentrations in the matte phase; "FeO", SiO_2, Cu and S concentrations in the slag phase; Fe/SiO_2 ratio and Fe^{3+}/($Fe^{2+} + Fe^{3+}$) ratio in the slag phase are illustrated in Fig. 3. The experimental and literature points are plotted along with the results of thermodynamic calculations carried out with the FactSage software [29] and the current version of the confidential thermodynamic database developed by Pyrosearch innovation centre (The University of Queensland) [12, 30].

The concentrations of Cu and S dissolved in the slag phase are dependent on the p(O_2) in the system and the concentrations of slagging elements (Ca, Al, Mg) present.

Analysis of the data also indicates that Al_2O_3 and MgO are distributed between the slag and spinel phases whereas CaO is only present in the slag phase. To illustrate distribution of Al_2O_3 and MgO between slag and spinel phases the logarithm of the ratio between measured Al_2O_3 (or MgO) wt.% concentration in slag phase and measured Al_2O_3 (or MgO) wt.% concentration in spinel phase was calculated and presented in Fig. 4a, b with error bars illustrating the standard deviation of the experimental data.
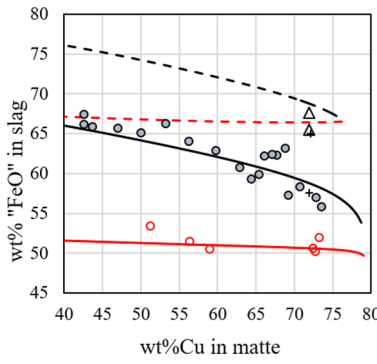
Discussion

O_2 and S_2 Partial Pressures

The relationships between matte grade and oxygen partial pressure at a fixed sulphur dioxide partial pressure of 0.25 atm are shown in Fig. 3a. The experimental data show the same tendency of increasing copper concentration in matte with increasing oxygen partial pressure that was observed earlier for the Cu–Fe–S–O–Si system without addition of Al_2O_3, CaO and MgO. This trend is consistent with thermodynamic predictions carried out using the current version of database, however, the oxygen partial pressure predicted to obtain a given matte grade is approximately 0.2 log units greater than observed for the range of matte compositions measured. Possible reasons for these differences have been previously discussed by Shishin et al. [11], but a clear explanation of this difference has yet to be established.
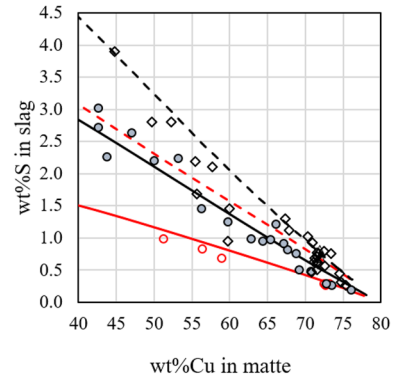
The model predictions indicate that the relationship between the oxygen partial pressure and the matte grade is almost independent of Al_2O_3, CaO and MgO at low concentrations of these components in slag phase. This appears to be the case both for equilibrium with spinel and for
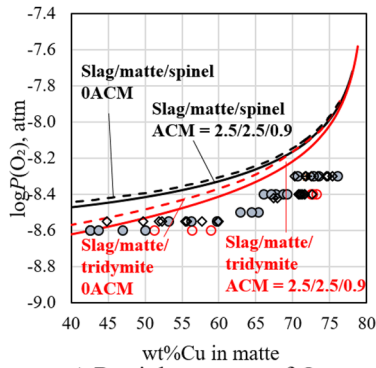
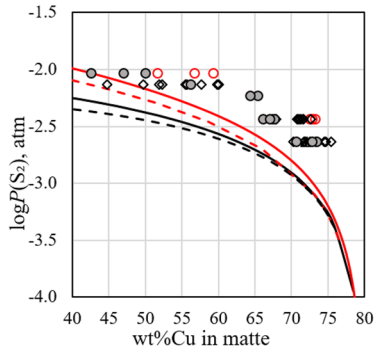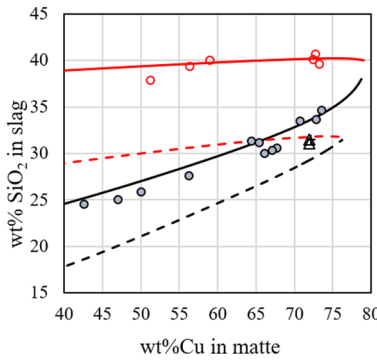a) Partial pressure of O_2

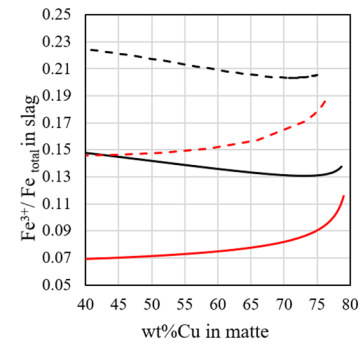b) Partial pressure of S_2

c) S in matte

d) O in matte

e) "FeO" in slag

f) SiO_2 in slag

g) Fe/SiO_2 in slag

h) Cu in slag

i) S in slag

j) Fe^{3+}/ Fe$_{total}$

Legend:
- ○ Current study, spinel, ACM = 2.5/2.5/0.9
- — FactSage calc, spinel, ACM=2.5/2.5/0.9
- --- FactSage calc, tridymite, ACM=0
- --- FactSage calc, spinel, ACM=0
- — FactSage calc, tridymite, ACM=4.5/2.5/0.9
- ○ Sineva et al. (2020), Slag/matte/p(SO2)=0.25/ tridymite, ACM=4.5/2.5/0.9, 1200 °C
- △ Sun et al. (2020) MgO effect, P(SO2) = 0.3 atm
- + Sun et al. (2020) CaO effect, P(SO2) = 0.3 atm
- ◇ Sineva et al. (2020) Individual CaO, Al2O3 and MgO effects, P(SO2) = 0.25 atm, spinel
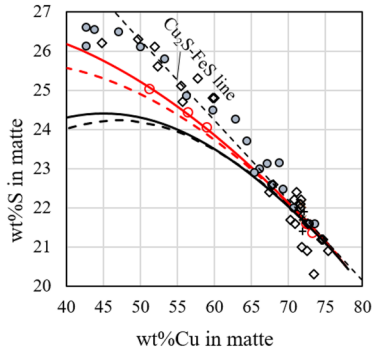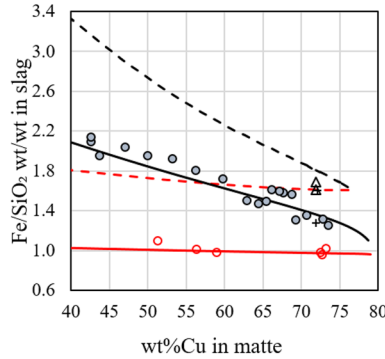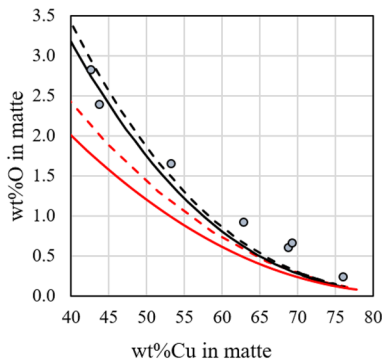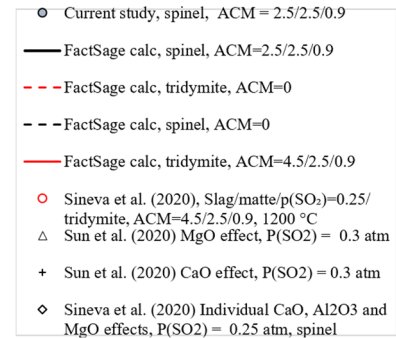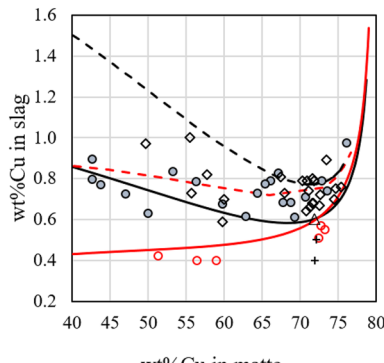
◄**Fig. 3** Gas/slag/matte/spinel equilibria in the Cu–Fe–O–S–Si–Al–Ca–Mg system at 1473 K (1200 °C) and $p(SO_2) = 0.25$ atm: **a** oxygen (O_2) partial pressure; **b** sulphur (S_2) partial pressure; **c** concentration of sulphur in matte; **d** dissolved oxygen in matte (measured directly by EPMA); **e** concentration of "FeO" in slag; **f** Fe/SiO$_2$ ratio; **g** concentration of Cu in slag; **h** concentration of sulphur in slag; **i** Fe^{3+}/Fe_{total} ratio in slag. Solid and dashed lines are calculated using FactSage 7.3 software and confidential thermodynamic database developed by Pyrosearch innovation centre (Shishin et al., 2018); symbols are experimental and literature data [20–23]. The abbreviation ACM in legend means the bulk concentrations (wt%) of Al_2O_3, CaO and MgO, respectively

equilibrium with tridymite. The results are consistent with previous measurements of slag/matte/tridymite phase equilibria in the Cu–Fe–O–S–Si system [20], also with study of individual effects of Al_2O_3, CaO and MgO on slag/matte/spinel phase equilibria [21, 32].

The predicted sulphur partial pressures decrease from $10^{-2.0}$ to $10^{-4.0}$ atm with increasing the matte grade between 40 and 80% Cu for $p(SO_2) = 0.25$ atm as shown in Fig. 3b. Sulphur partial pressure mainly depends on $P(SO_2)$ that was fixed in the system and inversely proportional to oxygen partial pressure. The effect of Al_2O_3, CaO and MgO on $p(S_2)$ is smaller compared to the above-mentioned effects.

Composition of the Matte Phase

The fluxing agents (Al_2O_3, CaO and MgO) are not present in the matte phase at measurable concentrations.

The sulphur concentration in the matte phase decreases with increasing copper concentration in matte, as illustrated in Fig. 3c. The experimental points follow the Cu_2S–FeS stoichiometric line at high matte grade area with copper concentration higher than 50 wt%, then change the slope due to increasing of oxygen and excess Fe metal solubility in mattes at low copper concentrations area. The thermodynamic predictions significantly underestimate the sulphur concentrations for low matte grades. This difference was also observed in other experimental studies of slag/matte/tridymite phase equilibria [21]. The mentioned discrepancy can be explained by overestimation of iron concentration in matte phase at low matte grade area. All these results indicate that further optimisation of thermodynamic database parameters for the matte solution is necessary. According to the calculated trends, matte in equilibrium with tridymite has higher sulphur concentration than matte equilibrated with spinel. This can be related to higher activity of "FeO" in the system. A qualitative comparison of the obtained results with the data of [25] showed the similar trends, but their experiments were carried out from 60 wt% Cu in matte and above. Therefore, the mentioned above discrepancy between experimental and calculated data at low-matte grades can not be confirmed by their experimental results.

The oxygen concentrations in the matte phase have been measured directly by EPMA and the results are presented in Fig. 3d. The concentration of oxygen in matte is evidently increasing with decreasing matte grade. It can be explained by higher concentration of iron in matte, which has higher chemical affinity to oxygen than copper. And finally, at very low matte grades (for instance, at Fe-S–O system) matte and slag will form a single oxysulphide solution [33, 34]. Good agreement between the experimental points and calculated trends is observed for 40–55 wt% copper concentration in matte, however, the experimental points are 0.2–0.4 wt% O higher than the calculated values at higher matte grades. The calculated oxygen concentrations in mattes in equilibrium with tridymite are lower than for mattes equilibrated with spinel that can be explained by lower oxygen partial pressure at fixed matte grade. The presence of Al_2O_3, CaO and MgO in the system has little effect on oxygen concentration in matte.

Composition of the Liquid Slag Phase

The "FeO" concentrations (Fig. 3e) and the Fe/SiO$_2$ ratios in the slag phase (Fig. 3f) for Al_2O_3, CaO and MgO-containing slags in equilibrium with spinel decrease with increasing matte grade. The experimental and predicted values agree well, and the FeO and Fe/SiO$_2$ ratios for a given matte grade are significantly lower than in ACM-free[3] slags. These trends are also consistent with the previously reported data for the systems in equilibrium with tridymite [20] also with data from [25]. The observed trends can be explained by dissolution of the fluxing agents in the slag and are associated with decrease of the activity coefficient of iron oxide in the slag phase. For slag equilibrated with tridymite, iron concentration in slag is almost constant over a wide matte grade area. However, in equilibrium with spinel the condition of spinel phase formation and keeping the liquid slag requires increasing of SiO_2 concentration in the slag phase that, in turn, results in decreasing of "FeO" concentration. The said statement is confirmed by Fig. 3f, illustrating constant Fe/SiO$_2$ ratio for tridymite-equilibrated slags and decreasing of the said ratio for spinel-equilibrated slags. Another proof is given in Table 2 and in Fig. 3f showing increasing the SiO_2 concentration in slags from 24.5 to 35.5 wt% at increasing of matte grade from 40 to 76 wt% Cu. In contrast, SiO_2 concentration in tridymite-equilibrated slag is almost constant over all matte grades range. Experimental data for SiO_2 concentration in slag are well correlated with thermodynamic prediction. With increasing matte grade, the compositions of slags in equilibrium with tridymite and with

---

[3] ACM-free is abbreviation that means slags do not contain Al_2O_3, CaO or MgO.

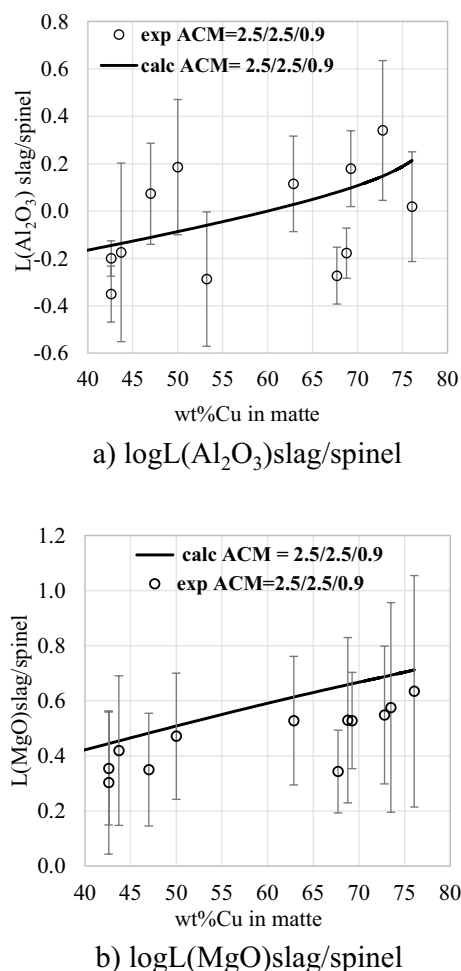a) logL(Al$_2$O$_3$)slag/spinel

b) logL(MgO)slag/spinel

Fig. 4 Gas/slag/matte/spinel equilibria in the Cu–Fe–O–S–Si–Al– Ca–Mg system at 1473 K (1200 °C) and p(SO$_2$) = 0.25 atm: **a** distribution coefficient of Al$_2$O$_3$ between slag and spinel; **b** distribution coefficient of MgO between slag and spinel. Solid lines are calculated using FactSage 7.3 software and confidential thermodynamic database developed by Pyrosearch innovation centre (Shishin et al., 2018); symbols denote experimental data

spinel approach each other. For ACM-free slags, the slag compositions become identical at 76 wt% of copper in matte.

Dissolved copper concentration in slag in equilibrium with spinel decreases with increasing matte grade from approximately 40 to 65% Cu and then increases for higher matte grades (Fig. 3g), resulting in a minimum copper concentration in slag for matte grades containing between approximately 65 and 70 wt% Cu. As it was mentioned above, at decreasing the matte grade chemical properties of slag and matte become closer with tendency of formation of one solution. Therefore, the mutual dissolution of copper and sulphur in slag, and oxygen in matte is increasing. For copper-enriched mattes with copper concentration higher than 70 wt%, increasing copper in slag can be explained by increase of copper activity in the system. The

presence of Al$_2$O$_3$, CaO and MgO decrease the concentration of copper in slag relative to ACM-free slags. For all matte grades, the copper concentrations in slag in equilibrium with spinel are higher than for tridymite-equilibrated slags. According to the calculated trends, for matte grades of 70 wt% Cu and higher, the copper concentration in slags is the same for both equilibria with tridymite and with spinel; however, the experimental results indicate that for these conditions copper concentrations in slag in equilibrium with tridymite are lower than for slag in equilibrium with spinel. Scatter of experimental data around 0.2 wt% is observed both for current results as well as literature data [21]. It can be explained by slightly different concentrations of ACM in the slag phase which are quite difficult to accurately adjust according to targeted values. Copper concentrations in slag measured by Sun et al. [22, 23] are 0.2–0.3 wt% lower that the results of the current study.

The concentrations of sulphur dissolved in slag in equilibrium with spinel and tridymite decrease with increasing matte grade as shown in Fig. 3h. The sulphur concentration in the slag in equilibrium with spinel at fixed matte grade is always higher than that in equilibrium with tridymite. The presence of Al$_2$O$_3$, CaO and MgO decreases the sulphur concentrations in slags in equilibrium with both tridymite and spinel phases. There is good agreement between the experimental points for slag/matte/spinel equilibria, the calculated values and literature data [20–23, 25]. The higher measured sulphur concentrations in paper [21] at fixed matte grade can be explained by lower ACM addition.

Only the calculated Fe^{3+}/Fe$_{total}$ ratios in slag are illustrated in Fig. 3i, as the experimental values have not been determined in this study. For slags in equilibrium with spinel, the ratio is predicted to decrease with increasing matte grade up to approximately 75 wt% Cu and then slightly increase at higher matte grades. This tendency can be explained by increasing concentration of SiO$_2$ in slag, as SiO$_2$ has a higher affinity to FeO than to Fe$_2$O$_3$. In contrast, the Fe^{3+}/Fe$_{total}$ ratios in slags in equilibrium with tridymite increase monotonically with increasing oxygen partial pressure in the system through the whole range of matte grades similar to changing of copper concentration in slag (Fig. 3 e). The presence of the fluxing agents in the system results in decreased Fe^{3+}/Fe$_{total}$ ratios relative to the ACM-free slags for equilibrium with both tridymite and spinel phases.

Al$_2$O$_3$, CaO and MgO concentrations in slag phase were targeted at 2.5, 2.5. and 0.9 wt% correspondingly. However, measured concentrations of these elements in slag phase are slightly differed from the targeted values. The calculated standard deviations of the measured flux concentrations from the targeted values were as follows: 2.5 ± 0.7 wt% for Al$_2$O$_3$, 2.5 ± 0.3 wt% for CaO and 0.9 ± 0.2 wt% for MgO.

Al$_2$O$_3$	Fe/SiO$_2$												
	1.10	1.15	1.20	1.25	1.30	1.35	1.40	1.45	1.50	1.55	1.60	1.65	1.70
0.0	6.1	4.5	3.1	1.8	0.5	0.0	0.0	0.0	0.0	0.0	0.0	0.0	0.0
0.5	4.9	3.4	2.0	0.6	0.0	0.0	0.0	0.0	0.0	0.0	0.0	0.0	0.0
1.0	3.8	2.3	0.9	0.0	0.0	0.0	0.0	0.0	0.0	0.0	0.0	0.0	0.0
1.5	2.7	1.2	0.0	0.0	0.0	0.0	0.0	0.0	0.0	0.0	0.0	0.0	0.0
2.0	1.6	0.1	0.0	0.0	0.0	0.0	0.0	0.0	0.0	0.0	0.0	0.0	1.5
2.5	0.6	0.0	0.0	0.0	0.0	0.0	0.0	0.0	0.0	0.0	0.0	1.7	4.0
3.0	0.0	0.0	0.0	0.0	0.0	0.0	0.0	0.0	0.0	0.0	1.7	4.0	6.3
3.5	0.0	0.0	0.0	0.0	0.0	0.0	0.0	0.0	0.0	1.4	3.8	6.1	8.3
4.0	0.0	0.0	0.0	0.0	0.0	0.0	0.0	0.0	1.0	3.4	5.8	8.0	10.1
4.5	0.0	0.0	0.0	0.0	0.0	0.0	0.0	0.4	2.9	5.3	7.6	9.8	11.9
5.0	0.0	0.0	0.0	0.0	0.0	0.0	0.0	2.2	4.7	7.0	9.3	11.4	13.5
5.5	0.0	0.0	0.0	0.0	0.0	0.0	1.4	3.9	6.4	8.7	10.9	13.0	15.0
6.0	0.0	0.0	0.0	0.0	0.0	0.5	3.1	5.6	7.9	10.2	12.4	14.4	16.4
6.5	0.0	0.0	0.0	0.0	0.0	2.2	4.7	7.1	9.4	11.6	13.8	15.8	17.8
7.0	0.0	0.0	0.0	0.0	1.2	3.8	6.3	8.6	10.9	13.0	15.1	17.1	19.0
7.5	0.0	0.0	0.0	0.2	2.8	5.3	7.7	10.0	12.3	14.4	16.4	18.3	20.2
8.0	0.0	0.0	0.0	1.8	4.3	6.8	9.1	11.4	13.6	15.6	17.6	19.5	21.4

Fig. 5 Calculated wt% solids (tridymite or spinel) in slag as function of Fe/SiO$_2$ and Al$_2$O$_3$ bulk concentration. Slag/matte equilibria at 1200 °C, p(SO$_2$) = 0.25 atm, 60 wt% Cu in matte, CaO = 2.5 wt%, MgO = 0.9 wt%

Composition of the Spinel Phase

It was noted earlier that both Al$_2$O$_3$ and MgO dissolve in the spinel phase, while CaO is concentrated in the slag phase. The main component of spinel is magnetite with concentration of Fe$_3$O$_4$ ranging from 94 to 98 wt% (see the resulting Table 2). Depending on the P(O$_2$) and total concentration of the corresponding compound in the system 0.7–3.6 wt% of Al$_2$O$_3$ and 0.1–0.35 wt% of MgO are dissolved in spinel phase. The graphs illustrating the distribution coefficients of Al$_2$O$_3$ and MgO between slag and spinel are shown in Fig. 4a, b. For experimental data high values of standard deviation are observed due to measurement uncertainties of Al$_2$O$_3$ and MgO concentrations in spinel phases. The distribution coefficients for both of these components increase with increasing matte grade by a factor of two at coper concentration in matte phase from 40 to 75 wt% Cu. Within the mentioned above experimental uncertainties calculated trends are in good agreement with experimental data.

Industrial Implications

Formation of solid phases (tridymite or spinel) in smelting furnaces results in increased effective viscosity of slag (slurry effect) and slows down the settlement of physically entrained droplets of matte. Uncontrolled amounts of solids may cause accretion formation and, in extreme cases, freezing of the furnace. A potential benefit of the solid phases present in the slag is decreased refractory wear due to lower

solubility of refractory components and formation of protective layer on the furnace walls. A common practice is operating the furnace at fixed Fe/SiO$_2$ in slag, based on extensive experience of operators. The optimized value is selected for a typical furnace feed. The trend towards increasing variability in feed composition is continuing and may even be accelerating due to changes in the mining industry, such as the depletion of high-grade ore reserves, the increasing use of alternative feed materials, such as recycled metals, electronic waste, etc. These secondary materials are often high in Al$_2$O$_3$ and Al. The addition of Al$_2$O$_3$ has a strong effect on spinel and tridymite liquidus, as shown in the present study and in previous studies [20, 21, 26]. To achieve optimum performance and output from the furnace, a change in process conditions will be required when a high-Al material enters the feed.

The calculated fluxing table shown in Fig. 5 demonstrates the effect of alumina concentration in the slag on the percentage of solid phases for a set Fe/SiO$_2$ ratio at 1200 °C, total pressure of 1 atm, p(SO$_2$) = 0.25 atm, 60 wt% Cu in matte, fixed CaO = 2.5 wt% and MgO = 0.9 wt%. The p(SO$_2$) = 0.25 atm in the calculation was selected to correspond to the experiments in the present study. In industrial practice, the effective p(SO$_2$) for slag/matte equilibria depends on the type of furnace. The value of "% Solids" is the mass ratio [m(Spinel) + m(Tridymite)] / [m(Liquid slag) + m(Spinel) + m(Tridymite)]·100%. Within the selected range, no other solid phases (e.g. mullite, wollastonite, feldspar) are predicted to form. The range of compositions for which the slag is fully liquid is highlighted in green between

Al$_2$O$_3$	Fe/SiO$_2$												
	1.10	1.15	1.20	1.25	1.30	1.35	1.40	1.45	1.50	1.55	1.60	1.65	1.70
0.0	0.51	0.52	0.53	0.54	0.55	0.56	0.57	0.58	0.60	0.61	0.62	0.64	0.65
0.5	0.51	0.52	0.53	0.54	0.55	0.56	0.57	0.58	0.59	0.61	0.62	0.63	0.65
1.0	0.51	0.52	0.53	0.54	0.55	0.56	0.57	0.58	0.59	0.60	0.62	0.63	0.64
1.5	0.51	0.52	0.53	0.53	0.54	0.55	0.57	0.58	0.59	0.60	0.61	0.63	0.64
2.0	0.50	0.51	0.52	0.53	0.54	0.55	0.56	0.57	0.59	0.60	0.61	0.62	0.62
2.5	0.50	0.51	0.52	0.53	0.54	0.55	0.56	0.57	0.58	0.59	0.61	0.60	0.58
3.0	0.50	0.51	0.51	0.52	0.53	0.54	0.55	0.57	0.58	0.59	0.58	0.56	0.55
3.5	0.49	0.50	0.51	0.52	0.53	0.54	0.55	0.56	0.57	0.57	0.55	0.53	0.52
4.0	0.49	0.50	0.50	0.51	0.52	0.53	0.54	0.56	0.56	0.54	0.52	0.51	0.49
4.5	0.48	0.49	0.50	0.51	0.52	0.53	0.54	0.55	0.53	0.51	0.50	0.48	0.47
5.0	0.48	0.49	0.49	0.50	0.51	0.52	0.53	0.52	0.51	0.49	0.48	0.46	0.45
5.5	0.47	0.48	0.49	0.50	0.51	0.52	0.51	0.50	0.48	0.47	0.45	0.44	0.43
6.0	0.47	0.47	0.48	0.49	0.50	0.51	0.49	0.48	0.46	0.45	0.43	0.42	0.41
6.5	0.46	0.47	0.48	0.49	0.50	0.48	0.47	0.46	0.44	0.43	0.42	0.40	0.39
7.0	0.45	0.46	0.47	0.48	0.48	0.46	0.45	0.44	0.42	0.41	0.40	0.39	0.38
7.5	0.45	0.46	0.46	0.47	0.46	0.44	0.43	0.42	0.41	0.39	0.38	0.37	0.36
8.0	0.44	0.45	0.46	0.45	0.44	0.43	0.41	0.40	0.39	0.38	0.37	0.36	0.35

Fig. 6 Calculated concentrations of dissolved copper in slag for the conditions shown in Fig. 4. Red lines show the limiting compositions for fully liquid slags (Color figure online)

the liquidus conditions corresponding to equilibrium with tridymite at low Fe/SiO$_2$ and spinel at high Fe/SiO$_2$ ratios. Effectively, increasing Al$_2$O$_3$ in slag moves the Fe/SiO$_2$ ratios for silica saturation to lower values; in contrast increasing Al$_2$O$_3$ in slag increases the likelihood of spinel formation for a given Fe/SiO$_2$ ratio.

Having developed an improved thermodynamic database describing the system it is possible to predict the effect of Al$_2$O$_3$ concentration and Fe/SiO$_2$ ratio on both the concentration of dissolved copper in slag and the % solids for a given matte grade. It can be seen from the example given in (Fig. 6) that the presence of Al$_2$O$_3$ in slag decreases the concentration of dissolved copper whereas increased Fe/SiO$_2$ ratio results in increased copper in slag. In Fig. 6, wt% Cu is defined as the mass ratio [m(Cu in spinel) + m(Cu in Liquid slag)/[m(Liquid slag) + m(Spinel) + m(Tridymite)]· 100%. The range of fully liquid slags is shown between the thick red lines.

Looking just at the concentration of copper in slag + solids (Fig. 6) without considering the mass of slag can lead to the wrong conclusion that as much as possible of Al$_2$O$_3$ and SiO$_2$ should be added during copper concentrate smelting to reduce copper losses. This is certainly not the case because copper losses are function of copper concentration in the slag and the mass of produced slag. Moreover, in industrial practice copper in slag is present in a form of dissolved copper and mechanically entrained matte droplets. Thermodynamic model of the present study provides a tool

to calculate the concentration of dissolved copper and the mass of slag. In the calculations above, the concentrate containing 28% Cu, 38% Fe and 33 wt% S, was smelted with a O$_2$-N$_2$ atmosphere. The amount of oxygen was increased in the modelling to achieve a target matte compositions, while p(SO$_2$) was fixed at 0.25 atm. The mass of SiO$_2$, Al$_2$O$_3$, MgO was adjusted to achieve the target slag compositions.

Conclusions

The integrated experimental and thermodynamic modelling approach has been applied to determine gas/slag/matte/spinel equilibria in the "Cu$_2$O"– "FeO"–SiO$_2$–S–Al$_2$O$_3$–CaO–MgO system under selected conditions at fixed p(SO$_2$) = 0.25 atm and controlled oxygen partial pressures at 1200 °C. The combined effects of Al$_2$O$_3$–CaO–MgO on the system have been characterised by measurement of the compositions of the slag, matte and spinel phases formed following equilibration of the system. The results have been compared with those in the ACM-free systems in equilibrium with spinel and tridymite.

The thermodynamic database accurately describes the equilibria in these complex systems, demonstrating the value of a rigorous thermodynamic approach to predicting process outcomes.

An example of the application of the thermodynamic database is given in the form of a fluxing table, a guide

that could be used by furnace operators to identify safe or optimum operating ranges in situations of varying slag compositions.

Data availability Data provided in the article are available on request.

Declarations

Conflict of interest On behalf of all authors, the corresponding author states that there is no conflict of interest.

References

1. Davenport WG, Schlesinger ME, King MJ, Sole KC (2002) Extractive metallurgy of copper, 4th edn. Elsevier, Amsterdam, pp 155–171

2. Yazawa A (1955) Fundamental studies on copper smelting. III. Partial liquidus diagram for Cu2S–FeS–FeO system. Technol Rep Tohoku Univ 19(2):239–250

3. Kameda M, Yazawa A (1961)The oxygen content of copper mattes. in physical chemistry of process metallurgy, part 2. In: TMS Confernce Proceesings, Interscience, New York

4. Kuxmann U, Bor FY (1965) Studies on the solubility of oxygen in copper mattes under ferric oxide slags saturated with silica. Erzmetall 18:441–450

5. Bor FY, Tarassoff P (1971) Solubility of oxygen in copper mattes. Can Metall Quat 10(4):267–271

6. Nagamori M (1975) Metal loss to slag: part I. Sulfidic and oxidic dissolution of copper in fayalite slag from low grade matte. Metall Mater Trans B 5(3):531–538. https://doi.org/10.1007/BF02644646

7. Shimpo R, Goto S, Ogawa O, Asakura I (1986) A study on the equilibrium between copper matte and slag. Can Metall Quat 25(2):113–121

8. Yazawa A, Nakazawa S, and Takeda Y (1983) Distribution Behavior of Various Elements in Copper Smelting Systems. in Adv. Sulfide Smelting. In: Proceegings of International Sulfide Smelting Symposium on Extractive. Processing Metallurgy Meet. Metall. Soc. AIME

9. Takeda Y (1997) Copper solubility in matte smelting slag. In: Proceedings of the 5th International Conference on Molten Slags, Fluxes, and Salts '97. Iron and Steel Society, Warrendale

10. Takeda Y (1997) Oxygen potential measurement of iron silicate slag-copper-matte system. In: Proceedings of the 5th International Conference on Molten Slags, Fluxes, and Salts '97. Iron and Steel Society, Warrendale

11. Shishin D, Decterov SA, Jak E (2018) Thermodynamic assessment of slag-matte-metal equilibria in the Cu–Fe–O–S–Si system. J Phase Equilib Diffus 39(5):456–475. https://doi.org/10.1007/s11669-018-0661-0

12. Shishin D, Hayes PC, Jak E (2018) Multicomponent thermodynamic databases for complex non-ferrous pyrometallurgical processes. In: Davis BR et al (eds) Extraction 2018. Springer, Ottawa. https://doi.org/10.1007/978-3-319-95022-8_68

13. Jak E, Shevchenko M, Shishin D, Hidayat T, Hayes PC (2020) Characterization of phase equilibria and thermodynamics with integrated experimental and modelling approach for complex lead primary and recycling processing. In: Siegmund A et al (eds) PbZn 2020: 9th International symposium on lead and zinc processing, San Diego, USA. Springer, Cham, pp 337–349. https://doi.org/10.1007/978-3-030-37070-1_30

14. Hidayat T, Fallah-Mehrjardi A, Hayes PC, Jak E (2020) The influence of temperature on the gas/slag/matte/spinel equilibria in the Cu–Fe–O–S–Si system at fixed P(SO₂) = 0.25 atm. Metall Mater Trans B. https://doi.org/10.1007/s11663-020-01807-x

15. Hidayat T, Fallah-Mehrjardi A, Hayes PC, Jak E (2018) Experimental investigation of gas/slag/matte/spinel equilibria in the Cu–Fe–O–S–Si system at 1473 K (1200 °C) and P(SO₂)=0.25 atm. Metall Mater Trans B 49(4):1750–1765. https://link.springer.com/article/10.1007/s11663-018-1262-3

16. Fallah-Mehrjardi A, Hidayat T, Hayes PC, Jak E (2019) Experimental investigation of gas/slag/matte/tridymite equilibria in the Cu–Fe–O–S–Si system in controlled gas atmospheres at 1200°C and P(SO₂)=0.1 atm. Int J Mater Res 110(6):489–495. https://doi.org/10.3139/146.111776

17. Fallah-Mehrjardi A, Hidayat T, Hayes PC, Jak E (2017) Experimental investigation of gas/slag/matte/tridymite equilibria in the Cu–Fe–O–S–Si system in controlled gas atmospheres: experimental results at T=1473 K [1200°C] and P(SO₂)=0.25 atm. Metall Mater Trans B 48(6):3017–3026. https://doi.org/10.1007/s11663-017-1076-8

18. Fallah-Mehrjardi A, Hidayat T, Hayes PC, Jak E (2017) Experimental investigation of gas/slag/matte/tridymite equilibria in the Cu–Fe–O–S–Si system in controlled gas atmospheres: development of technique. Metall Mater Trans B 48(6):3002–3016. https://doi.org/10.1007/s11663-017-1073-y

19. Fallah-Mehrjardi A, Hidayat T, Hayes PC, Jak E (2018) Experimental investigation of gas/slag/matte/tridymite equilibria in the Cu–Fe–O–S–Si system in controlled gas atmosphere: experimental results at 1523 K (1250 °C) and P(SO₂) = 0.25 atm. Metall Mater Trans B 49(4):1732–1739. https://doi.org/10.1007/s11663-018-1260-5

20. Sineva S, Fallah-Mehrjardi A, Hidayat T, Shevchenko M, Shishin D, Hayes PC, Jak E (2020) Experimental investigation of gas/slag/matte/tridymite equilibria in the Cu–Fe–O--S–Si–Al–Ca–Mg system in controlled gas atmosphere: experimental results at 1473 K (1200 °C), 1573 K (1300 °C) and p(SO₂) = 0.25 atm.

J Phase Equilib Diffus 41(3):243–256. https://doi.org/10.1007/s11669-020-00810-8

21. Sineva S, Fallah-Mehrjardi A, Hidayat T, Hayes PC, Jak E (2020) Experimental study of the individual effects of Al_2O_3, CaO and MgO on gas/slag/matte/spinel equilibria in Cu–Fe–O–S–Si–Al–Ca–Mg system at 1473 K (1200°C) and $p(SO_2)$ = 0.25 atm. J Phase Equilib Diffus 41(6):859–869. https://doi.org/10.1007/s11669-020-00847-9

22. Sun Y, Chen M, Ballares E, Pizarro C, Contreras L, Baojun Z (2020) Effect of CaO on the liquid/spinel/matte/gas equilibria in the Si–Fe–O–Cu–S system at controlled $P(SO_2)$ 0.3 and 0.6 atm. Calphad. https://doi.org/10.1016/j.calphad.2020.101751

23. Sun Y, Chen M, Ballares E, Pizarro C, Contreras L, Baojun Z (2020) Effect of MgO on the liquid/spinel/matte/gas equilibria in the Si–Fe–Mg–O–Cu–S system at controlled $P(SO_2)$ 0.3 and 0.6 atm. Calphad 70:1018–1023. https://doi.org/10.1016/j.calphad.2020.101803

24. Chen M, Sun Y, Ballares E, Pizarro C, Baojun Z (2019) Experimental studies of liqud/spinel/matte/gas equilibria ib the Si–Fe–O–Cu–S system at controlled $p(SO_2)$ 0.3 and 0.6 atm. Calphad 66:1016–1042. https://doi.org/10.1016/j.calphad.2019.101642

25. Chen M (2022) Phase equilibria and precious or high-tech metal distributions in copper smelting systems. Doctoral Thesis, Aalto University

26. Shishin D, Hidayat T, Fallah-Mehrjardi A, Hayes PC, Decterov SA, Jak E (2018) Integrated experimental and thermodynamic modelling study of the effects of Al_2O_3, CaO and MgO on slag–matte equilibria in the Cu–Fe–O–S–Si–(Al, Ca, Mg) system. J Phase Equilib Diff 40(4):445–461. https://doi.org/10.1007/s11669-019-00716-0

27. Shevchenko M, Nicol S, Hayes PC, Jak E (2018) Experimental liquidus studies of the Pb–Cu–Si–O system in equilibrium with metallic Pb–Cu alloy. Metall Mater Trans B 49(4):1690–1698. https://doi.org/10.1007/s11663-018-1249-0

28. Shevchenko M, Jak E (2018) Experimental liquidus studies of the Pb–Fe–Si–O system in equilibrium with metallic Pb. Metall Mater Trans B 49(1):159–180. https://doi.org/10.1007/s11663-017-1136-0

29. Bale CW et al (2016) FactSage thermochemical software and databases, 2010–2016. Calphad 54:35–53. https://doi.org/10.1016/j.calphad.2016.05.002

30. Shishin D, Hayes PC, Jak E (2019) Development and applications of thermodynamic database in copper smelting. In: 58th Annual Conference of Metallurgists Copper'2019. Vancouver, Canada: MetSoc

31. Shevchenko M, Jak E (2019) Experimental liquidus studies of the Pb–Fe–Si–O system in air. J Phase Equilib Diff 40(3):319–355. https://doi.org/10.1007/s11669-019-00727-x

32. Sineva S, Hidayat T, Fallah-Mehrjardi A, Starykh R, Hayes PC, Jak E (2021) Experimental investigation of gas-matte-spinel and gas-slag-matte-spinel equilibria in the Cu–Fe–O–S–Si system at 1200°C: effect of SO_2 partial pressure. Miner Process Extr Metall. https://doi.org/10.1080/25726641.2021.1919375

33. Shishin D, Jak E, Decterov SA (2015) Critical assessment and thermodynamic modeling of the Fe–O–S system. J Phase Equilib Diffus 36(3):224–240. https://doi.org/10.1007/s11669-015-0376-4

34. Shishin D, Jak E, Decterov SA (2015) Thermodynamic assessment and database for the Cu–Fe–O–S system. Calphad 50:144–160. https://doi.org/10.1016/j.calphad.2015.06.004

Authors and Affiliations

Svetlana Sineva[1] · Denis Shishin[1] · Maksym Shevchenko[1] · Peter C. Hayes[1] · Evgueni Jak[1]

Denis Shishin
d.shishin@uq.edu.au

Maksym Shevchenko
m.shevchenko@uq.edu.au

Peter C. Hayes
p.hayes@uq.edu.au

Evgueni Jak
e.jak@uq.edu.au

[1]   Pyrometallurgy Innovation Centre (PYROSEARCH), The University of Queensland, Brisbane, QLD 4072, Australia